

RSC Advances



This is an *Accepted Manuscript*, which has been through the Royal Society of Chemistry peer review process and has been accepted for publication.

Accepted Manuscripts are published online shortly after acceptance, before technical editing, formatting and proof reading. Using this free service, authors can make their results available to the community, in citable form, before we publish the edited article. This *Accepted Manuscript* will be replaced by the edited, formatted and paginated article as soon as this is available.

You can find more information about *Accepted Manuscripts* in the [Information for Authors](#).

Please note that technical editing may introduce minor changes to the text and/or graphics, which may alter content. The journal's standard [Terms & Conditions](#) and the [Ethical guidelines](#) still apply. In no event shall the Royal Society of Chemistry be held responsible for any errors or omissions in this *Accepted Manuscript* or any consequences arising from the use of any information it contains.

1 **One-pot synthesis of thiol- and amine-bifunctionalized mesoporous silica and**
2 **applications in uptake and speciation of arsenic**

3

4 Peng Li, Xiao-qin Zhang, Yi-jun Chen, Tian-yi Bai, Hong-zhen Lian*, Xin Hu*

5 *State Key Laboratory of Analytical Chemistry for Life Science, School of Chemistry &*

6 *Chemical Engineering and Center of Materials Analysis, Nanjing University, 22*

7 *Hankou Road, Nanjing, 210093, China*

8

9 * Corresponding authors. Tel.: +86 25 83686075; fax: +86 25 83325180. *E-mail*

10 *address:* hzlian@nju.edu.cn (H.Z. Lian); Tel.: +86 25 83592247; fax: +86 25

11 83325180. *E-mail address:* huxin@nju.edu.cn (X. Hu)

12

13

14 **Abstract**

15 A series of thiol- and amine-bifunctionalized mesoporous silicas were synthesized

16 by one-pot co-condensation of tetraethyorthosilicate,

17 3-mercaptopropyltrimethoxysilane and

18 N-(2-aminoethyl)-3-aminopropyltriethoxysilane. The mesoporous materials were

19 characterized by X-ray diffraction, scan electron microscopy, transmission electron

20 microscopy, nitrogen gas adsorption, infrared spectroscopy, thermogravimetric

21 analysis and elemental analysis. As(V) and As(III) were effectively adsorbed by

22 amine and thiol on the functionalized silica, respectively, through electrostatic

23 interaction and chelation. Adsorption isotherms and kinetic uptake profiles of As(V)
24 and As(III) onto these adsorbents were investigated by batch adsorption experiments.
25 On the other hand, this material was employed for speciation analysis of arsenic using
26 a homemade syringe-based solid phase extraction device. As(V) and As(III) were
27 effectively separated and preconcentrated in a single run through a sequential elution
28 strategy, in which 0.1 M HNO₃ was used to selectively elute As(V) first and then 1 M
29 HNO₃ with 0.01 M KIO₃ to elute As(III). The merits of easy preparation, low cost,
30 high adsorption capacity and selective desorption, make the bifunctional mesoporous
31 silica an ideal solid material for removal and speciation analysis of arsenic in
32 environmental waters.

33 **Key words:** Bifunctional mesoporous silica, one-pot reaction, arsenic adsorption,
34 speciation analysis, solid phase extraction

35

36

37 1. Introduction

38

39 In recent decades, heavy metal contamination to natural waters is of great concern
40 because of the toxicities of heavy metals in relatively low concentrations and
41 tendency towards bioaccumulation to plants, animals and human beings.^{1,2} It is thus of
42 necessity to control the harmful effects of heavy metal ions through daily monitoring
43 and removal technologies. Solid material, also as adsorbent, used for adsorption of
44 heavy metal ions has received increasingly more attentions in recent years since it is

45 simple, low-cost and easy to be automated.³ Moreover, it can be easily incorporated
46 into automated solid phase extraction (SPE) procedures for determination of trace
47 metal ions and their species.⁴ A variety of adsorbents, such as biomass,⁵ carbon,⁶
48 zeolites,⁷ and functionalized inorganic supports⁸ have been applied to trace elements
49 area with satisfactory results. In contrast with some other solid materials, a great deal
50 of attention has been paid to mesoporous silica due to its large specific surface area,
51 good dispersibility and controllable morphology.^{9,10} Recently, Wang et al.¹¹ prepared a
52 L-cysteine-functionalized SBA-15 for Hg(II) sorption, which shows a large
53 adsorption capacity. Awual et al.¹² synthesized
54 6-((2-(2-hydroxy-1-naphthoyl)hydrazono)methyl)benzoic acid (HMBA)
55 functionalized material as optical mesoporous adsorbent for selective recognition and
56 removal of ultra-trace Cu(II) and Pd(II) ions.

57 Up till now, a series of functionalized mesoporous silicas, generally synthesized by
58 post modification of pure mesoporous silica gel or direct co-condensation of
59 organosilane reagents with tetra-alkoxysilanes (either tetraethoxysilane (TEOS) or
60 tetramethoxysilane (TMOS)), are available to adsorb heavy metal ions. Three main
61 types of functional groups (amine, thiol and carboxylic) have been demonstrated to be
62 the specific ligands for most of metal ions.¹³⁻¹⁵ However, there is a difference for
63 some elements, e.g., arsenic, selenium, antimony and tellurium, because they exist in
64 different species in environmental water, and property of each species is quite
65 different.¹⁶ Take arsenic as an example, it is an omnipresent toxic trace element and is
66 mainly found in environmental water with two oxidation states, As(III) and As(V).

67 Since the different properties of these two species, it is hard to adsorb them
68 simultaneously through mono-functionalized mesoporous silica like thiol- or
69 amine-functionalized.^{8,17-19} In addition, it is worth noting that most of the adsorbents
70 including mesoporous silica are facing the similar problem, so a pre-oxidation or
71 pre-reduction operation is indispensable for uptake both arsenic species. For example,
72 a pre-oxidization of As(III) to As(V) is usually involved using oxidizing agents or
73 photocatalytic oxidation to enhance As(III) removal.^{20,21}

74 The studies have shown that the toxic effect of arsenic in an environmental or
75 biological system depends critically on its chemical form, and As(III) is the most toxic
76 form of the water-soluble species while As(V) is also relatively toxic. Thus, it is not
77 only important to remove As(III) and As(V), but also necessary for quantitative
78 determination of each arsenic species in daily monitoring.²²⁻²⁹ Conventionally, the
79 speciation of inorganic arsenic without employing chromatographic separation can be
80 achieved by selective adsorption of one species onto adsorbents, and the other species
81 was calculated by subtraction with total inorganic arsenic. To obtain the total
82 inorganic arsenic content, an additional extraction procedure was usually needed after
83 pre-oxidization/pre-reduction of arsenic in sample,²⁴⁻²⁷ or adjustment of sample
84 pH,^{28,29} which make the sample pretreatment a bit time-consuming.

85 For the removal or speciation analysis of arsenic, the conversion of species from
86 one form to another may not only cause operational complexity, but also introduce
87 interferences. In this paper, we report the first attempt to synthesize a thiol- and
88 amine-bifunctionalized mesoporous silica by one-step method for simultaneous

89 uptake of As(III) and As(V). The novel material synthesized under different reactant
90 proportions between organosilane reagents and TEOS was characterized by using
91 X-ray diffraction (XRD), scan electron microscopy (SEM), transmission electron
92 microscopy (TEM), N₂ adsorption, Fourier-transform infrared spectroscopy (FT-IR),
93 thermogravimetric analysis (TGA) and elemental analysis (EA). The batch adsorption
94 experiments were performed to investigate their adsorption behaviors and capacities
95 for As(III) and As(V). Then, by means of a facilely homemade syringe-based SPE
96 device, a sequential elution strategy for arsenic speciation analysis was proposed, and
97 simultaneous separation and preconcentration of As(III) and As(V) was achieved in a
98 single run without any change of sample conditions.

99

100

101 **2. Experimental**

102

103 **2.1 Reagents and materials**

104

105 Cetyltrimethylammonium bromide (CTAB) was purchased from TCI (Tokyo,
106 Japan). Tetraethyorthosilicate (TEOS) and 3-mercaptopropyltrimethoxysilane
107 (MPTMS) were purchased from Alfa Aesar (Tianjing, China), and
108 N-(2-aminoethyl)-3-aminopropyltriethoxysilane (AAPTES) was purchased from
109 Ourchem (Shanghai, China). HNO₃ was of guarantee reagent and obtained from
110 Merck (Zurich, Switzerland). All other chemicals were at least of analytical grade, and

111 used without further purification. Deionized water (DIW, 18.25 M Ω cm) obtained
112 from a Milli-Q water system (Millipore, Bedford, MA, USA) was used throughout the
113 experiment.

114 Stock standard solutions of As(III) and As(V), 1000.0 mg L⁻¹, were prepared by
115 respectively dissolving appropriate amounts of Na₃AsO₃ and As₂O₅ (both of analytical
116 grade, purchased from Johnson Matthey, UK) in DIW. Lower concentration standard
117 solutions were prepared daily by appropriate dilutions from their stock solutions.

118

119 **2.2 Synthesis of bifunctional mesoporous silica**

120

121 Bifunctional mesoporous silica was synthesized via co-condensation of TEOS,
122 MPTMS and APTES with surfactant (CTAB) as the template in alkaline solution
123 (Scheme 1). Typically, 120 mL DIW and 3.5 mL NaOH (1 M) were added to 0.5 g
124 CTAB and stirred at 80 °C for 30 min. Then, (1-2*X*) \times 12.5 mmol of TEOS, *X* \times 12.5
125 mmol of MPTMS and *X* \times 12.5 mmol of APTES were mixed and added to the above
126 clear basic surfactant solution. Following the injection, a white precipitation was
127 observed within 4 min. The reaction mixture was allowed to stir at 80 °C for 2 h under
128 the atmosphere of nitrogen, and then the resulting slurry was filtered and rinsed with
129 excess H₂O, followed by ethanol and naturally dried overnight. Afterwards, the dried
130 solid was extracted with a mixed solution of 0.5 mL HCl and 150 mL ethanol by
131 stirring at 50 °C for 3 h. The extraction was repeated twice to accomplish complete
132 removal of CTAB. Then, the solid was filtered and washed with copious amounts of

133 water until neutral, and subsequently rinsed repeatedly with ethanol. The resulting
134 mesoporous silica was finally dried under vacuum for 24 h.

135 The molar composition of the reaction mixture was $(1-2X)$ TEOS : X MPTMS : X
136 AAPTES : 0.11 CTAB : 0.28 NaOH : 532 H₂O, where the reaction molar proportion
137 between MPTMS/AAPTES and total Si is represented by X . Four different $X = 0$,
138 0.025, 0.075 and 0.15 were taken, and the bifunctionalized mesoporous silica
139 materials thus obtained are hereafter noted as MP-AAP-0%, MP-AAP-2.5%,
140 MP-AAP-7.5% and MP-AAP-15%, respectively.

141

142 **Scheme 1**

143

144 **2.3 Characterization of bifunctional mesoporous silica**

145

146 XRD, SEM, TEM, N₂ adsorption, FT-IR, TGA and EA were employed for the
147 characterization of the synthesized bifunctional mesoporous silica. Powder XRD
148 experiment was performed on the Philip X'Pert Pro using a Cu K α radiation source.
149 Low angle diffraction with a 2-theta range of 1 to 10° was used to investigate the
150 long-range order of the materials. Particle morphology of these materials was
151 obtained by SEM using a Hitachi S-3400N II with 10 kV accelerating voltage and
152 0.005 nA of beam current for imaging. The microstructure was characterized by a
153 high resolution transmission electron microscopy (HRTEM) on a JEM-200CX
154 microscope operating at a 200 kV accelerating voltage. N₂ adsorption measurement

155 was carried out on a Micromeritics ASAP 2020 BET surface analyzer system at liquid
156 N₂ temperature (-196 °C). Before measurement, the sample was outgassed at 90 °C for
157 1 h and then at 150 °C for 4 h. The data were evaluated using the
158 Brunauer-Emmett-Teller (BET) and Barrett-Joyner-Halenda (BJH) methods to
159 calculate the surface area and pore volumes/pore size distributions, respectively.
160 FT-IR spectra were recorded on a Nicolet-6700 spectrometer in the range of 4000-450
161 cm⁻¹. TGA of the materials was performed on a Perkin-Elmer Pyris 1 DSC from 303
162 to 973 K with a heating rate of 10 K min⁻¹. EA of the particles was carried out on an
163 Elementar Vario EL III using oxygen as the combustion gas.

164

165 **2.4 Batch adsorption experiments**

166

167 The adsorption of As(III) and As(V) on the bifunctional mesoporous silica was
168 measured in batch experiments by adding a fixed amount of adsorbent (0.010 g) into a
169 definite volume (10 mL) of either As(III) or As(V) solution. Initial pH of the solutions
170 was adjusted with diluted HNO₃ or NH₃·H₂O by using a pH meter. The mixture was
171 placed in a rotary mixer and shaken (100 rpm) at room temperature for 30 min. After
172 centrifugation, the remaining arsenic in the supernatant liquid was quantified using an
173 inductively coupled plasma atomic emission spectrometer (ICP-AES, Perkin-Elmer,
174 Model Optima 5300DV) by measuring the signal intensity at the emission wavelength
175 of As 189.042 nm. The amount of arsenic adsorbed was calculated using the following
176 equation:

177 $Q_e = [(C_o - C_e) * V] / m$

178 Where C_o and C_e are the original and equilibrium concentrations, respectively, in
179 the solution of the arsenic species (mg L^{-1}), V is the solution volume (mL), and m is
180 the adsorbent mass (mg).

181

182 **2.5 Speciation analysis procedure**

183

184 Syringe filter tip ($0.45 \mu\text{m}$) of 13 mm in diameter was used to form a simple SPE
185 device. Briefly, 200 mg mesoporous silica were dispersed into 10 mL DIW, the
186 suspension was then inhaled into a 10 mL syringe cylinder and was injected averagely
187 into ten syringe filter tips sequentially and rapidly. In this case, DIW was passed
188 through the filter membrane while the silica particles were collected on the surface of
189 the filter membrane. As a result, a layer of 20 mg silica particles was immobilized in
190 each syringe filter tip.

191 In the extraction step, 10 mL As(III) or As(V) solution was allowed to flow through
192 the filter tip at a flow rate of 1 mL min^{-1} for preconcentration of As(III) and As(V).
193 The flow rate was precisely controlled by a pump (Baoding Longer, Model BT100) or
194 roughly controlled by pushing the syringe by hand. The effluent was collected and
195 ^{75}As was monitored by an inductively coupled plasma mass spectrometer (ICP-MS,
196 Perkin-Elmer, Model Elan-9000) to calculate the adsorption percentage. In the elution
197 step, 1.5 mL of $0.1 \text{ mol L}^{-1} \text{ HNO}_3$ was injected into the filter to desorb As(V) from the
198 silica firstly and the eluent was collected. Then, 1.5 mL of 1 M HNO_3 with 0.01 M

199 KIO_3 was injected into the filter to desorb As(III) and the eluent was also collected.
200 Finally, two portions of the eluent were directly introduced into ICP-MS for
201 determination of As(V) and As(III), respectively.

202

203

204 **3. Results and discussion**

205

206 **3.1 Structure, property and function of the bifunctional silica**

207

208 3.1.1 Structural and morphological characterization of the bifunctional silica

209 The mesoporous structure and morphology of the bifunctionalized silica particles
210 were studied using XRD, TEM, SEM and N_2 adsorption.

211 Small-angle XRD patterns of the final materials with different initial reactant ratios
212 are shown in Fig. 1. The well-resolved diffraction patterns characteristic of hexagonal
213 MCM-41 silica, including (1 0 0), (1 1 0) and (2 0 0) peaks, were observed in
214 MP-AAP-0%, MP-AAP-2.5% and MP-AAP-7.5%, while MP-AAP-15% appeared to
215 be disordered. The peak intensity of the samples weakens as the organosilane dosage
216 increases, implying that the organosilane in the synthesis mixture would perturb the
217 self-assembly of surfactant micelles and the silica precursors. Meanwhile, a
218 systematic shift of the diffraction peaks to larger 2θ angles with increasing
219 organosilane contents suggests that slight lattice contractions occur as a result of the
220 incorporation of the organosilane groups within the mesostructure synthesis (Table 1).

221

222 **Fig. 1**

223

224 The particle morphology and mesoporous structure of the resulting materials were
225 analyzed by SEM and TEM. The SEM micrographs in Fig. 2A show a dramatically
226 transformation of the particle morphology, with ellipsoidal particles being observed at
227 low concentration of organosilane reagents (MP-AAP-0% and 2.5%) and elongated
228 rods being observed at higher concentration of organosilane reagents
229 (MP-AAP-7.5%). The TEM micrographs of Fig. 2B revealed that the mesopores are
230 uniformly aligned along the long axes of MP-AAP-0%, MP-AAP-2.5% and
231 MP-AAP-7.5%. However, there were no ordered pores observed on the irregular
232 particles for MP-AAP-15%, which is consistent with the result from XRD observation
233 shown in Fig. 1.

234

235 **Fig. 2**

236

237 The N₂ adsorption analyses were performed on the synthesized materials. As shown
238 in Fig. 3, MP-AAP-0%, 2.5% and 7.5% display a type IV isotherm, while the
239 isotherm of MP-AAP-15% is different probably due to its out-of-order structure. The
240 surface area, pore volume and pore size distribution of the bifunctional materials are
241 listed in Table 1. It was found that the overall trend is that of a decrease in these
242 parameters with the increase of the initial organosilanes (*X*).

243

244 **Fig. 3**

245

246 3.1.2 Characterization of the functional groups on the bifunctional silica

247 FT-IR, TGA, and EA of N and S were carried out to confirm the organic functional
248 groups on the bifunctional mesoporous materials. FT-IR spectra of the obtained four
249 materials were acquired as shown in Fig. 4. The intensity of characteristic absorption
250 of C-N bond around 1480 cm^{-1} , C-H stretching in the range of $2850\text{-}3000\text{ cm}^{-1}$ and
251 S-H bond at 2575 cm^{-1} (inset) increases with increasing organic loading content,
252 which demonstrates the successful incorporation of N and S containing functional
253 groups in the matrix. N and S contents of the bifunctional silicas determined by EA
254 are listed in Table 1. As can be seen, the larger X results in more N and S in products.

255

256 **Fig. 4**

257

258 TGA (Fig. 5) shows that the weight loss of MP-AAP- X materials in the temperature
259 range between 473 and 923 K was 6.1%, 10.5%, 13.8% and 22.2% for MP-AAP-0%,
260 MP-AAP-2.5%, MP-AAP-7.5% and MP-AAP-15%, respectively, which are attributed
261 to the decomposition of the organic functional groups. The results were in accordance
262 with the FT-IR and EA.

263

264 **Fig. 5**

265

266 **Table 1**

267

268 **3.2 Batch adsorption behaviors of the bifunctional mesoporous silica**

269

270 3.2.1 Influence of pH on adsorption

271 Solution pH determines the distribution of arsenic species and surface property of
272 the bifunctional mesoporous silica, thereby influencing arsenic adsorption onto the
273 adsorbent. The effect of solution pH on the adsorption behaviors of As(III) and As(V)
274 is presented in Fig. 6. It is clear to see that As(III) and As(V) adsorption by the
275 bifunctional silica was sensitive to solution pH. The affinity of the bifunctional silica
276 to As(V) is mainly due to the strong electrostatic interaction of the protonated amine
277 group towards anionic arsenate species, which is the dominant species of As(V) in the
278 pH range of 3.0-7.0.²⁶ Whereas, the affinity to As(III) can be explained by the strong
279 chelation of mercapto group to As(III).^{29,30} So, the bifunctional material has the
280 simultaneous or selective adsorption ability for As(V) and As(III) within different pH
281 range. In addition, MP-AAP-0%, i.e., the pure SiO₂, shows no appreciable adsorption
282 to any of the two arsenic species.

283

284 **Fig. 6**

285

286 3.2.2 Adsorption equilibrium isotherm

287 To obtain adsorption equilibrium isotherm data, adsorption experiments were
288 performed using a fixed adsorbent/liquid ratio and varied concentrations of either
289 As(III) or As(V) solution. The obtained adsorption isotherms of As(V) and As(III) are
290 shown in Figs. 7A and B, respectively. According to Langmuir adsorption isotherm
291 models, the adsorption capacities (Q_m) for As(III) and As(V) were calculated and
292 listed in Table 1. From the results, for the four as-prepared bifunctional materials with
293 the elevation of the X value from 0 to 15%, the uptake of As(III) increased from 0 to
294 $192 \mu\text{mol g}^{-1}$, and the uptake of As(V) increased from 0 to $417 \mu\text{mol g}^{-1}$. At the same
295 time, we noted that Q_m for As(III) increased slowly when X increased from 7.5% to
296 15%. It might be because more mercapto groups are embedded in the co-condensation
297 and less percentage of the active mercapto groups are exposed to As(III) species,
298 which consequentially leads to a decrease in the As(III)/-SH molar ratio. In addition,
299 the adsorption of As(III) on MP-AAP-7.5% at pH 1.0 revealed that the strong
300 interaction between As(III) and the material cannot be destroyed by diluted acid.

301 Fig. 7C displays the As(V) and As(III) uptake curves for the two bifunctional
302 materials, MP-AAP-7.5% and MP-AAP-15%. It can be seen that two adsorbents
303 exhibit similar performance in the time. The adsorption for As(V) was finished in 30 s,
304 while for As(III) was in 5 min. As in the previous section of characterization of the
305 adsorbents, the difference between MP-AAP-7.5% and MP-AAP-15% is the degree of
306 mesoporous structure order and surface area. However, despite the high surface areas
307 and uniform mesoporosities of the adsorbents, the results do not demonstrate any
308 remarkably rapid arsenic uptake by the mesostructure.

309

310 **Fig. 7**

311

312 3.2.3 Adsorption capacity

313 A comparison of the adsorption capacity with the previous functionalized silica
314 materials reported for arsenic was made, and the results are listed in the Table 2. As
315 could be seen, the adsorption capacity of the bifunctionalized mesoporous silica
316 synthesized via one-pot co-condensation method is comparable with those obtained
317 by other reported adsorbents.

318

319 **Table 2**

320

321 **3.3 Speciation analysis of arsenic species**

322

323 3.3.1 Characteristics of the homemade SPE tip

324 Conventionally, SPE adsorbents were usually filled into a polymer or glass tube
325 plugged with a small portion of glass wool at both ends to construct a SPE
326 microcolumn or cartridge. The fabrication of microcolumn or cartridge is a little
327 tedious, and the reproduction between different batches is a little difficult. More
328 important, the back pressure of these devices is very high, especially using the small
329 size adsorbents at large flow rate. Syringe filter tip, which is ubiquitous in the
330 laboratory, was employed for a simple SPE device in the present study. Fig. 8 is the

331 schematic diagram of this device using for the separation of arsenic species.
332 MP-AAP-7.5% was used as the adsorbent due to its uniform structure, large surface
333 area and high adsorption capacity. As described in the experimental section, the
334 fabrication procedure of SPE tip is very simple. Furthermore, experiment results
335 indicated the SPE device possessing advantages, such as high permeability, low
336 pressure and facile assembly.

337

338 3.3.2 Preconcentration and elution

339 According to the results of batch experiments, As(V) and As(III) could be
340 simultaneously concentrated on the bifunctional adsorbent in a certain pH.
341 Considering the adsorption capacity, a pH of 4.0 was selected to guarantee
342 quantitative adsorption of As(III) and As(V) at the same time. The effect of sample
343 flow rate on the adsorption was examined by ejecting 10 mL sample solution
344 containing $100 \mu\text{g L}^{-1}$ As(V) or As(III) through the prepared SPE tip with different
345 sample flow rate. It was found that a quantitative adsorption for As(V) and As(III)
346 could be obtained when the sample flow rate was below 4 mL min^{-1} and 1 mL min^{-1} ,
347 respectively. So a sample flow rate of 1 mL min^{-1} controlled by pump or hands was
348 adopted for speciation analysis. For sampling volume, a handheld syringe-based SPE
349 was achieved and sensitive ICP-MS was used for detection of arsenic, so a volume of
350 10 mL of sample solution was taken for easy operation and appropriate detection level.
351 However, the sensitivity could be further increased by increasing the sampling
352 volume.

353 As described in the previous section, As(III) can be adsorbed on the bifunctional
354 silica both at pH 1.0 and 4.0, suggesting 0.1 M HNO₃ (pH 1.0) does not affect the
355 adsorption of As(III) on the adsorbent. In the view of As(V), the adsorption was much
356 affected by pH, especially the adsorption percentage decreased to 0% at pH 1.0. A
357 sequential elution strategy for As(III) and As(V) was proposed therefore, in which 0.1
358 M HNO₃ was employed to selectively elute As(V) first and then 1 M HNO₃ with 0.01
359 M KIO₃ was employed to elute As(III). The probable elution mechanism is that As(V)
360 is transformed from anion to uncharged species (H₃AsO₄) in 0.1 M HNO₃ and loses
361 electrostatic interaction with the adsorbent, and then mercapto groups are oxidized by
362 KIO₃ and the chelation between mercapto and As(III) is destroyed. Using individual
363 As(V) or As(III) solution, it was found that As(V) can be eluted quantitatively by
364 using 1.5 mL 0.1 M HNO₃, and no As(III) was observed in this process, and then,
365 As(III) can be eluted quantitatively by 1.5 mL 1 M HNO₃ with 0.01 M KIO₃. These
366 results confirmed the feasibility of the sequential elution strategy.

367

368 3.3.3 Interference study

369 Commonly encountered co-existing ions in environmental waters, e.g., alkali,
370 alkaline and transition metal ions may cause interferences on the preconcentration and
371 determination of arsenic. The influences of these ions were investigated by using 10
372 $\mu\text{g L}^{-1}$ As(V) and As(III). It was found that the main ions existing in water such as Na⁺,
373 K⁺, Ca²⁺, Mg²⁺ and Cl⁻ can be tolerated at least 1000 mg L⁻¹. For the potential ions
374 which may compete with arsenic for thiol and amine sites, 5 mg L⁻¹ Al³⁺, Fe³⁺ and

375 Zn^{2+} , $100 \mu\text{g L}^{-1}$ Sb(III), Se(IV) and Hg^{2+} did not cause obvious change to results in
376 the determination of As(V) and As(III). Therefore, the proposed method could be
377 applied for speciation analysis of inorganic arsenic in environmental waters.

378

379 3.3.4 Analytical performance and its validation

380 With a sampling volume of 10 mL and desorbing volume of 1.5 mL, the obtained
381 limits of detection (LODs, defined as 3-fold signal-to-noise ratio) were $0.015 \mu\text{g L}^{-1}$
382 for As(V) and $0.025 \mu\text{g L}^{-1}$ for As(III), which were much lower than the allowed limit
383 of arsenic in environmental waters. The calibration curves were established in the
384 range of $0.1\text{-}100 \mu\text{g L}^{-1}$ As(V) and As(III) with linear equation of $y = 12039.4x +$
385 507.1 ($R^2 = 0.999$) and $y = 13841.8x + 1494.0$ ($R^2 = 0.998$), respectively. The
386 precisions (Relative standard deviations, RSDs) for six replicate determinations of 10
387 $\mu\text{g L}^{-1}$ As(V) and As(III) were 5.6% and 4.5%, respectively. Adsorbent
388 (MP-AAP-7.5%) prepared within batch ($n = 4$) and between different batches ($n = 3$)
389 was examined by measuring the recoveries of the same solution containing $10 \mu\text{g L}^{-1}$
390 As(V) and As(III) under the optimized conditions. It was found that the RSDs of
391 eluted As(V) and As(III) were 4.0% and 6.9% for intra-batch, and were 4.3% and 4.7%
392 for inter-batch, respectively.

393 The accuracy of the proposed separation scheme was evaluated by analyzing
394 standard solution and two certified reference materials, namely GSBZ 50004-88
395 (Standard environmental water sample) and GSB 080230 (Standard seawater sample).
396 The results of these analyses are summarized in Table 3. As can be seen, the

397 concentrations of As(V), As(III) and As(Total) were in good agreement with the
398 standard or certified values. These results indicated that As(III), As(V) and As(Total)
399 in these water samples can be successfully determined based on simultaneous
400 retention of As(Total) on the SPE tip, and sequential elution with appropriate eluent.

401

402 Table 3

403

404 In addition, if the levels of monomethylarsenic acid (MMA) and dimethylarsenic
405 acid (DMA) are need to be considered, a tandem SPE method that combined the
406 MP-AAP-7.5% with strong cation-exchange resin (SCX 732, Sinopharm Chemical
407 Reagent Co., Ltd) was investigated (Fig. 8B). The first SPE unit was filled with SCX,
408 and the second SPE unit was filled with MP-AAP-7.5%. After loading sample
409 solution, the tandem syringe filter tips were separated. The first one was eluted by 1
410 M HNO₃ for the retained DMA, and the second one was eluted orderly by 50 mM
411 acetic acid (HAc) for MMA, 0.1 M HNO₃ for As(V) and 1 M HNO₃ with 0.01 M
412 KIO₃ for As(III). The recoveries in ranges of 97-104%, 83-92%, 92-101% and 96-108%
413 were obtained for 10 mL of 10 µg L⁻¹ DMA, MMA, As(V) and As(III), respectively.

414

415 Fig. 8

416

417

418 4. Conclusions

419

420 Thiol- and amine-bifunctionalized mesoporous silica was for the first time
421 synthesized by one-pot co-condensation of TEOS, MPTMS and AAPTES under basic
422 CTAB solution. The amounts of MPTMS and AAPTES in the initial synthetic mixture
423 were varied, and their effects on the structural and chemical properties of these porous
424 materials were investigated systematically. Due to the different interaction
425 mechanisms between arsenic with bifunctional groups, As(V) and As(III) can be
426 simultaneously adsorbed by the adsorbents in a wide pH range, and their separation
427 can be realized by selective and sequential elution of As(V) with diluted 0.1 M HNO₃
428 and then As(III) with 1 M HNO₃ with 0.01 M KIO₃. The homemade syringe-based
429 SPE device possessing the characteristics such as portability and simplicity provides a
430 promising application for field sampling and pretreatment. These advantages make the
431 bifunctional mesoporous silica to be an attractive and desirable adsorbent not only for
432 arsenic removal from contaminated water, but also for arsenic speciation analysis.

433 Further investigations on the adsorption of other heavy metal ions on the
434 bifunctionalized mesoporous silica have been conducted to fully evaluate the property
435 of this adsorbent, which will be reported elsewhere.

436

437

438 **Acknowledgements**

439

440 This work was supported by National Natural Science Foundation of China
441 (21275069, 90913012), National Basic Research Program of China (973 program,
442 2009CB421601, 2011CB911003), National Science Funds for Creative Research
443 Groups (21121091), and Analysis & Test Fund of Nanjing University.

444

445

446 **References**

447

- 448 1 S. Babel and T. A. Kurniawan, *J. Hazard. Mater.*, 2003, **97**, 219-243.
- 449 2 F. L. Fu and Q. Wang, *J. Environ. Manage.*, 2011, **92**, 407-418.
- 450 3 T. M. Mututuvvari and C. D. Tran, *J. Hazard. Mater.*, 2014, **264**, 449-459.
- 451 4 B. Hu, F. Zheng, M. He and N. Zhang, *Anal. Chim. Acta*, 2009, **650**, 23-32.
- 452 5 X. W. Chen, A. M. Zou, M. L. Chen, J. H. Wang and P. K. Dasgupta, *Anal. Chem.*,
453 2009, **81**, 1291-1296.
- 454 6 M. L. Chen, Y. M. Lin, C. B. Gu and J. H. Wang, *Talanta*, 2013, **104**, 53-57.
- 455 7 W. Qiu and Y. Zheng, *J. Hazard. Mater.*, 2007, **148**, 721-726.
- 456 8 S. Mandal, T. Padhi and R. K. Patel, *J. Hazard. Mater.*, 2011, **192**, 899-908.
- 457 9 J. Aguado, J. M. Arsuaga, A. Arencibia, M. Lindo and V. Gascón, *J. Hazard.*
458 *Mater.*, 2009, **163**, 213-221.
- 459 10 B. G. Trewyn, I. I. Slowing, S. Giri, H. T. Chen and V. S. Lin, *Acc. Chem. Res.*,
460 2007, **40**, 846-853.
- 461 11 Q. Li, Z. Wang, D. M. Fang, H. Y. Qu, Y. Zhu, H. J. Zou, Y. R. Chen, Y. P. Du and

- 462 H. L. Hu, *New J. Chem.*, 2014, **38**, 248-254.
- 463 12 M. R. Awual, I. M. Rahman, T. Yaita, M. A. Khaleque and M. Ferdows, *Chem.*
464 *Eng. J.*, 2014, **236**, 100-109.
- 465 13 D. Rahmi, Y. Takasaki, Y. Zhu, H. Kobayashi, S. Konagaya, H. Haraguchi and T.
466 Umemura, *Talanta*, 2010, **81**, 1438-1445.
- 467 14 L. Zhang, W. Zhang, J. Shi, Z. Hua, Y. Li and J. Yan, *Chem. Commun.*, 2003, **0**,
468 210-211.
- 469 15 Y. L. Wang, L. J. Song, L. Zhu, B. L. Guo, S. W. Chen and W. S. Wu, *Dalton*
470 *Trans.*, 2014, **43**, 3739-3749.
- 471 16 Z. Mester, R. Sturgeon and J. Pawliszyn, *Spectrochim. Acta B*, 2001, **56**, 233-260.
- 472 17 D. Mohan and C. U. Pittman Jr, *J. Hazard. Mater.*, 2007, **142**, 1-53.
- 473 18 E. McKimmy, J. Dulebohn, J. Shah and T. J. Pinnavaia, *Chem. Commun.*, 2005, **0**,
474 3697-3699.
- 475 19 H. T. Fan, T. Sun, H. B. Xu, Y. J. Yang, Q. Tang and Y. Sun, *Desalination*, 2011,
476 **278**, 238-243.
- 477 20 T. Nakajima, Y. H. Xu, Y. Mori, M. Kishita, H. Takanashi, S. Maeda and A. Ohki,
478 *J. Hazard. Mater.*, 2005, **120**, 75-80.
- 479 21 A. H. Fostier, M.d. S. S. Pereira, S. Rath and J. R. Guimarães, *Chemosphere*,
480 2008, **72**, 319-324.
- 481 22 X. C. Le, X. Lu and X. F. Li, *Anal. Chem.*, 2004, **76**, 26 A-33 A.
- 482 23 T. Llorente-Mirandes, J. Calderón, F. Centrich, R. Rubio and J.F. López-Sánchez,
483 *Food Chem.*, 2014, **147**, 377-385.

- 484 24 X. P. Yan, X. B. Yin, X. W. He and Y. Jiang, *Anal. Chem.*, 2002, **74**, 2162-2166.
- 485 25 X. P. Yan, R. Kerrich and M. J. Hendry, *Anal. Chem.*, 1998, **70**, 4736-4742.
- 486 26 D. H. Chen, C. Z. Huang, M. He and B. Hu, *J. Hazard. Mater.*, 2009, **164**,
- 487 1146-1151.
- 488 27 M. L. Chen, C. B. Gu, T. Yang, Y. Sun and J. H. Wang, *Talanta*, 2013, **116**,
- 489 688-694.
- 490 28 C. Z. Huang, B. Hu and Z. C. Jiang, *Spectrochim. Acta B*, 2007, **62**, 454-460.
- 491 29 E. Boyacı, A. Çağır, T. Shahwan and A. E. Eroğlu, *Talanta*, 2011, **85**, 1517-1525.
- 492 30 A. Howard, M. Volkan, D. Y. Ataman, *Analyst*, 1987, **112**, 159-162.
- 493
- 494

495 **Table legends**

496

497 **Table 1** Physicochemical characteristics of the bifunctional silicas

498 **Table 2** Comparison of adsorption capacity with other silica based functionalized

499 adsorbents

500 **Table 3** Analytical results of As(V) and As(III) in standard solutions and certified

501 materials

502

503

504 **Figure captions**

505

506 **Fig. 1** XRD patterns of MP-AAP-0% (a), 2.5% (b), 7.5% (c) and 15% (d).

507 **Fig. 2** SEM (A) and TEM (B) images of MP-AAP-0%, 2.5%, 7.5% and 15%.

508 **Fig. 3** (A) N₂ adsorption-desorption isotherms and (B) Pore size distribution of
509 MP-AAP-0%, 2.5%, 7.5% and 15%.

510 **Fig. 4** FT-IR spectra of MP-AAP-0% (a), 2.5% (b), 7.5% (c) and 15% (d).

511 **Fig. 5** TG curves of MP-AAP-0% (a), 2.5% (b), 7.5% (c) and 15% (d).

512 **Fig. 6** Influence of solution pH on the adsorption of As(III) and As(V) onto
513 MP-AAP-0% and 7.5%.

514 **Fig. 7** Adsorption isotherms of As(V) (A) and As(III) (B) onto MP-AAP-0%, 2.5%,
515 7.5% and 15%, solution pH=4.0. Adsorption kinetics (C) of As(V) and As(III) onto
516 MP-AAP-7.5% and 15%, solution pH=4.0.

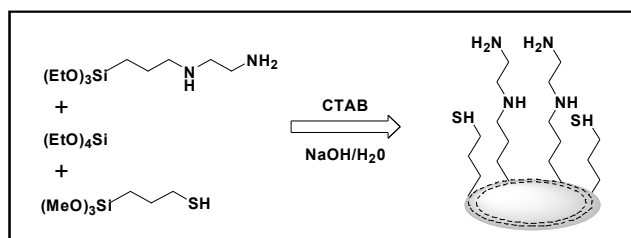
517 **Fig. 8** Schematic diagram of the SPE procedure for speciation analysis. (A) Single
518 SPE tip for inorganic arsenic. (B) Tandem SPE tips for main organic and inorganic
519 arsenic.

520

521

522 **Scheme**

523



524

525 **Scheme 1** Preparation of the bifunctional mesoporous silica of MP-AAP-X.

526 **Tables**

527

528 **Table 1** Physicochemical characteristics of the bifunctional silicas

Adsorbent	Initial X	d spacing (nm)	SBET (m^2 g^{-1})	Pore size (nm)	Pore volume (cm^3 g^{-1})	EA ($\mu\text{mol g}^{-1}$)		Q _m ($\mu\text{mol g}^{-1}$)	
						Sulfur	Nitrogen	As(III)	As(V)
MP-AAP-0%	0	4.0	992	3.5	0.87	0	0	0	0
MP-AAP-2.5%	0.025	3.9	940	3.2	0.73	199	536	33	49
MP-AAP-7.5%	0.075	3.8	706	2.0	0.35	739	807	139	156
MP-AAP-15%	0.15	3.4	547	<2.0	0.34	1912	1500	192	417

529

530 **Table 2** Comparison of adsorption capacity with other silica based functionalized
531 adsorbents

Adsorbent	Adsorption capacity (mg g ⁻¹)		Ref.
	As(V)	As(III)	
MP-AAP-2.5%	3.7	2.5	This work
MP-AAP-7.5%	11.7	10.4	
MP-AAP-15%	31.3	14.4	
Mercapto-functionalized mesoporous silica	--	19.4	[18]
AAPTS modified silica gel	13.9	--	[19]
AAPTS modified mesoporous silica	10.3	--	[26]
(NH ₂ +SH) modified silica gel	0.29	2.7	[29]

532

533

534 **Table 3** Analytical results of As(V) and As(III) in standard solutions (ST) and
 535 certified materials

Sample	Certified ($\mu\text{g L}^{-1}$)			Found ($\mu\text{g L}^{-1}$)		
	As(V)	As(III)	As(Total)	As(V)	As(III)	As(Total)
ST1	10	10	20	10.8 \pm 0.7	11.0 \pm 0.9	21.8 \pm 1.6
ST2	100	100	200	98.6 \pm 7.8	107.5 \pm 8.6	216.1 \pm 16.4
50004-88	--	--	124 \pm 8	2.1 \pm 0.8	128.5 \pm 9.6	130.6 \pm 10.5
080230	--	--	1000 \pm 40	70.4 \pm 16.6	945.3 \pm 73.4	1015.7 \pm 80.0

536

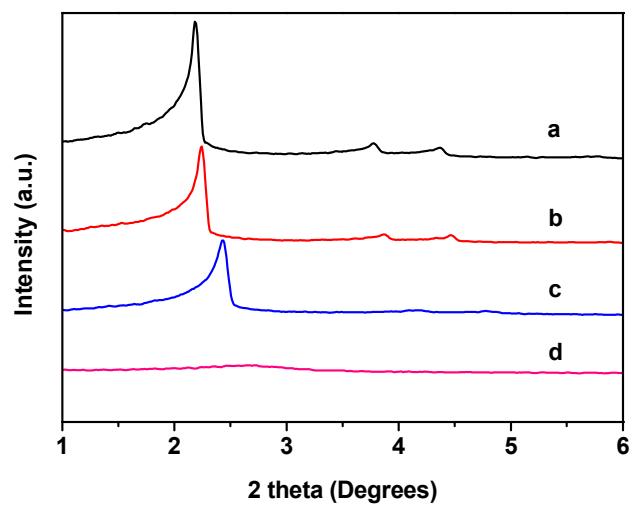
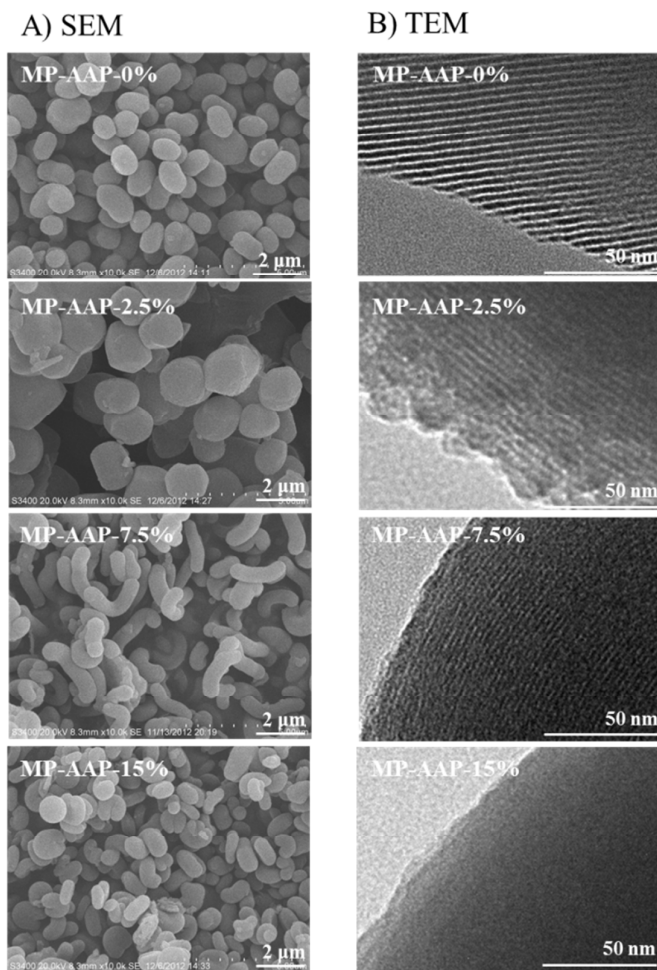


Fig. 1

**Fig. 2**

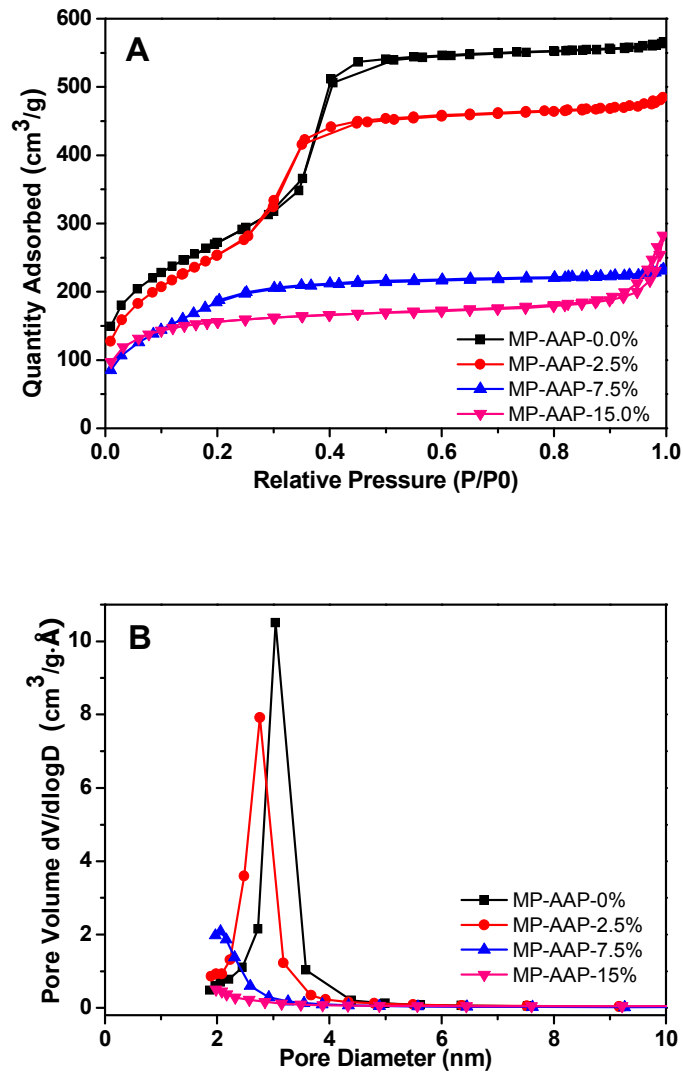


Fig. 3

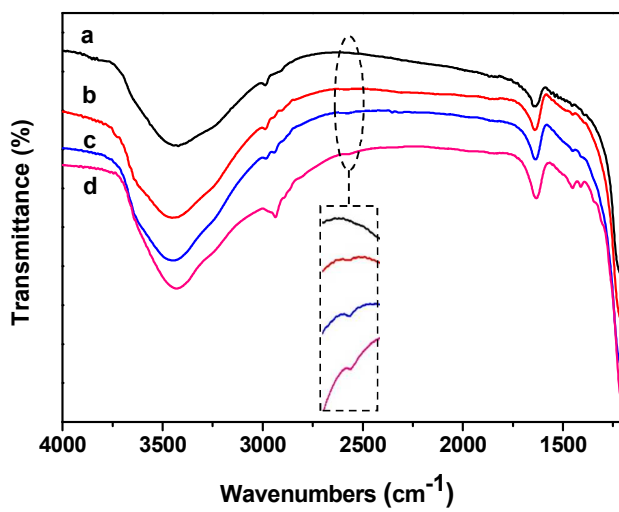


Fig. 4

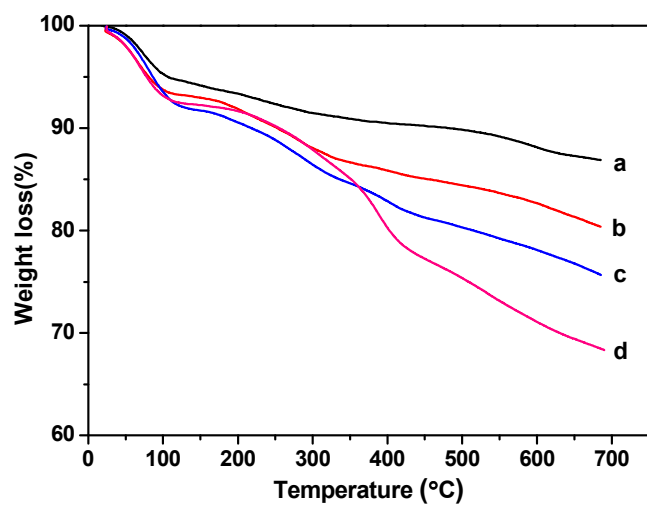


Fig. 5

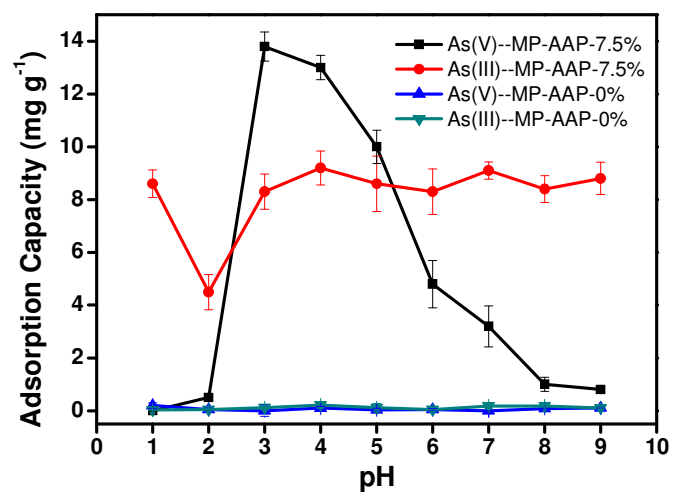
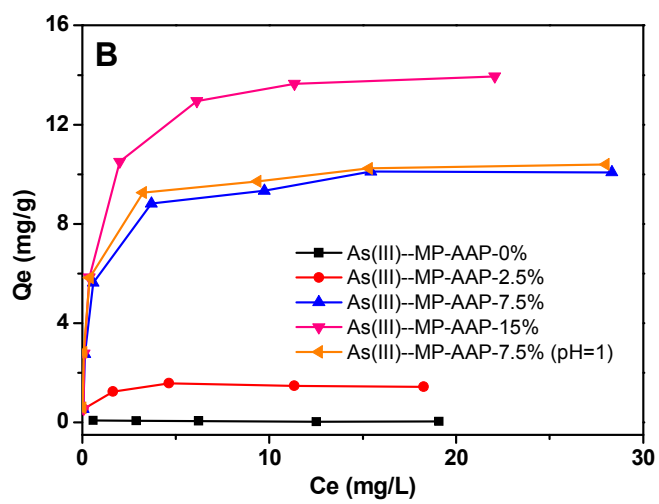
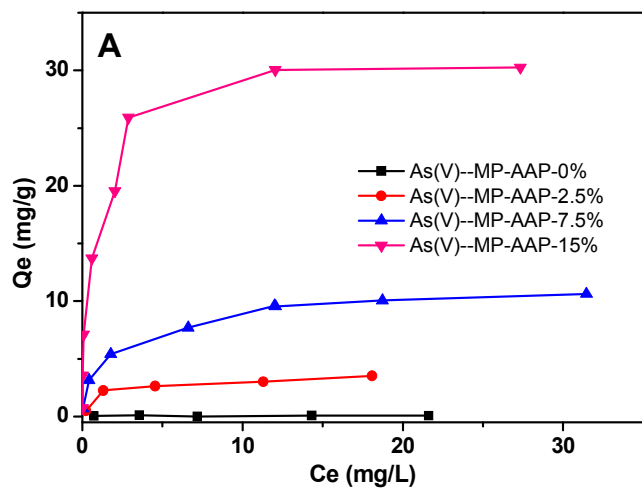


Fig. 6



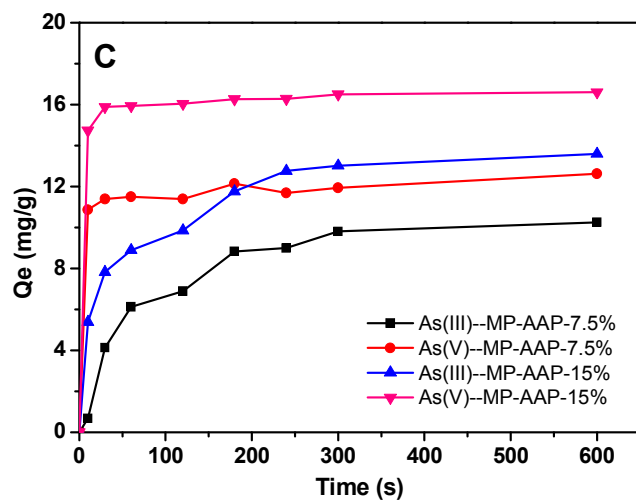


Fig. 7

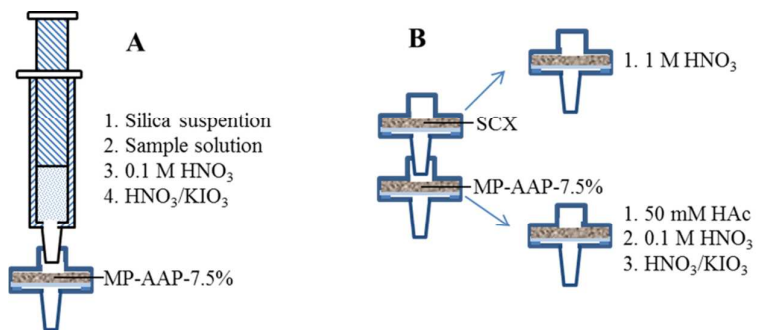
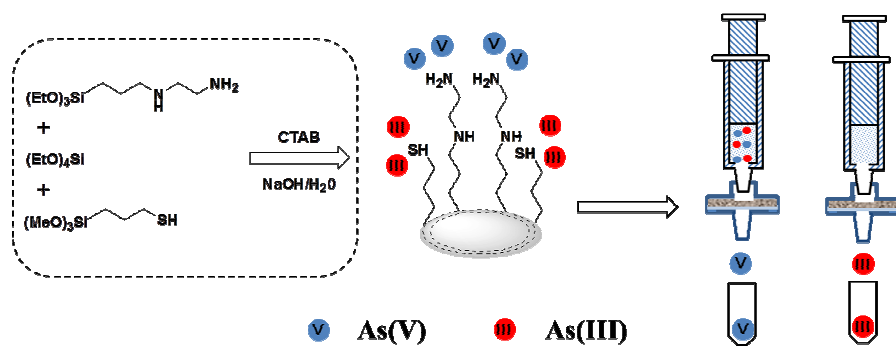


Fig. 8

Graphical Abstract



Removal and separation of As(V) and As(III) can be achieved by the bifunctional silica.